Published in Comput. Optim. Appl. 49 (2011), no. 1, 101–122

AUGMENTED LAGRANGIAN FOR CONE CONSTRAINED TOPOLOGY OPTIMIZATION

SAMUEL AMSTUTZ

Abstract. Algorithmic aspects for the solution of topological shape optimization problems subject to a cone constraint are addressed in this paper. In this framework, an augmented Lagrangian method based on the concept of topological derivative is proposed. It is illustrated by some numerical experiments in structural optimization with compliance and eigenfrequency constraints and multiple loads.

1. Introduction

This paper deals with the construction of numerical methods for the topological optimization of domains in the presence of constraints. The problem of interest can be stated as follows. Let D be a domain of $\mathbb{R}^d$, $d = 2$ or $d = 3$ (computational domain), $\mathcal{E}$ be a set of subdomains of D, and K be a closed convex cone of a Banach space Y. We are given two functionals

$$\begin{array}{rccc} J: & \mathcal{E} & \to & \mathbb{R}, \\ & \Omega & \mapsto & J(\Omega), \end{array} \qquad \begin{array}{rccc} G: & \mathcal{E} & \to & Y, \\ & \Omega & \mapsto & G(\Omega). \end{array}$$

Our purpose is to solve the minimization problem

$$\min_{\Omega \in \mathcal{E}_{ad}} J(\Omega), \tag{1.1}$$

where the feasible set is defined by

$$\mathcal{E}_{ad} = \{\Omega \in \mathcal{E},\ G(\Omega) \in -K\}.$$

Several methods have been developed to approximate this problem by a differentiable optimization problem, that can be handled by standard optimization algorithms. The most popular one, at least as far as industrial applications are concerned, is the parametric shape optimization method, which takes the CAD parameters as design variables (see, *e.g.*, [2] and the references therein). It enables in particular a straightforward implementation of second order methods, like Newton's method or the SQP algorithm. However the set of attainable domains is restricted by the parametrization. In order to enlarge this set, many authors appeal to relaxation methods, like the homogenization [13, 1] or SIMP [14, 24]. These methods have the converse drawback: they lead to unfeasible domains, made of intermediate or composite material. Finally, one has to mention the shape derivative approach [25, 31], which is based on the sensitivity analysis with respect to boundary perturbations. Nevertheless, as the differentiation is not computed with respect to the global design variables, the algorithmic issue remains nontrivial, especially in the constrained case [20]. In addition, topology variations are not permitted in this context. More flexibility can be obtained by combining the shape derivative and a level-set domain representation [5, 32].

In this paper, we follow another approach which relies on the topological sensitivity analysis [21, 23, 29, 22, 26, 30, 9, 8]. The topological derivative, also called topological gradient, of a shape functional J at some point x of the domain is a number $g(x)$ which measures the first variation of J with respect to a topology perturbation localized around x, typically the nucleation of a small hole. In the unconstrained situation, the nonnegativity of $g(x)$ at every point of Ω is an obvious necessary minimality condition. Some algorithms have been devised on the basis of the solution of this condition by means of fixed point type methods [23, 10]. Some others combine the shape and topological derivatives within a level-set formalism [3, 16]. By construction, all these algorithms allow topology changes without introducing unfeasible material. In the cone constrained case described above, one proves that a necessary optimality condition can be written in terms of the nonnegativity of

Key words and phrases. topological sensitivity, topological derivative, topology optimization, augmented Lagrangian, cone constraint.

the topological derivative of a Lagrangian functional, together with a complementarity condition [11]. The present paper aims at providing algorithms dedicated to the solution of this optimality condition. We focus on first order methods, since the first order topological derivative of the Lagrangian does not have to vanish at the optimum.

The paper is organized as follows. The notations concerning the topology perturbations and the associated topological derivatives are specified in Section 2. The optimality conditions are recalled in Section 3. In Sections 4, we prove that local optima correspond to local saddle points of the Lagrangian. We show in Section 5 that the augmented Lagrangian enjoys similar properties. Therefore we propose in Section 6 to adapt the Uzawa algorithm to these two Lagrangians. Section 7 is devoted to a first series of numerical examples dealing with structural optimization with compliance and eigenfrequency constraints. Other examples in the context of multiple loads are treated in Section 8.

2. Topological sensitivity

Starting from an arbitrary domain $\Omega \in \mathcal{E}$ and given

- a family of points $z = (z_1, ..., z_N) \in (D \setminus \partial\Omega)^N$, $N \in \mathbb{N}$,
- a family of radii $\rho = (\rho_1, ..., \rho_N) \in \mathbb{R}_+^N$,

we define the perturbed domain

$$\Omega_{z,\rho} = \Omega \cup \bigcup_{z_i \in D \setminus \overline{\Omega}} B(z_i, \rho_i) \setminus \bigcup_{z_i \in \Omega} \overline{B(z_i, \rho_i)},$$

with $B(z_i, \rho_i) = \{x \in \mathbb{R}^d, |x - z_i| < \rho_i\}$ and $|.|$ the canonical Euclidean norm of $\mathbb{R}^d$. To assure that the perturbed domain remains in $\mathcal{E}$ as soon as the radii are small enough, it may be necessary to restrict the centers to some subset $\mathcal{T}(\Omega)$ of $D \setminus \partial\Omega$. Thus we assume that, for all family $z = (z_1, ..., z_N) \in \mathcal{T}(\Omega)$, there exists $\rho_0 > 0$ such that

$$\rho \in [0, \rho_0]^N \Rightarrow \Omega_{z,\rho} \in \mathcal{E}.$$

The first variation of the objective and constraint functionals with respect to such perturbations is expressed by the following assumption.

Assumption 2.1. For every domain $\Omega \in \mathcal{E}$, there exist two functions $J'(\Omega) : D \to \mathbb{R}$ and $G'(\Omega) : D \to Y$ as well as a homeomorphism f of $\mathbb{R}_+$ into itself with $f(0) = 0$ such that, for all $(z, \rho) \in \mathcal{T}(\Omega)^N \times \mathbb{R}_+^N$, $N \in \mathbb{N}$, the following asymptotic expansions hold:

$$J(\Omega_{z,\rho}) - J(\Omega) = \sum_{i=1}^{N} f(\rho_i) J'(\Omega)(z_i) + o(f(\rho_1), ..., f(\rho_N)),$$

$$G(\Omega_{z,\rho}) - G(\Omega) = \sum_{i=1}^{N} f(\rho_i) G'(\Omega)(z_i) + o(f(\rho_1), ..., f(\rho_N)). \tag{2.1}$$

We refer the reader, *e.g.*, to the papers [23, 29, 22, 26, 9, 8] for some examples of such expansions. These papers focus on a single perturbation ($N = 1$), but the additive behavior is natural and it is proved in some cases (see, *e.g.*, [30, 11, 12]).

For convenience we introduce the cone $\mathcal{Q}(\Omega)$ of all functions $\varphi : \mathcal{T}(\Omega) \to \mathbb{R}_+$ with finite support, *i.e.*, for which the set $\{x \in \mathcal{T}(\Omega), \varphi(x) \neq 0\}$ consists of a finite number of points. For all $\varphi \in \mathcal{Q}(\Omega)$ and all function ψ defined in $\mathcal{T}(\Omega)$ with values in an arbitrary set, we define the pairing

$$[\psi, \varphi] = \sum_{z \in \mathcal{T}(\Omega)} \varphi(z)\psi(z).$$

Also, we define for all $\varphi \in \mathcal{Q}(\Omega)$ the domain

$$\Omega_\varphi = \Omega \cup \bigcup_{z \in D \setminus \overline{\Omega}} B(z, f^{-1} \circ \varphi(z)) \setminus \bigcup_{z \in \Omega} \overline{B(z, f^{-1} \circ \varphi(z))}.$$

We derive straightforwardly the following proposition.

Proposition 2.2. *For all $\eta \in \mathcal{Q}(\Omega)$ and all $t > 0$ sufficiently small, we have*

$$J(\Omega_{t\eta}) - J(\Omega) = t[J'(\Omega), \eta] + o(t), \tag{2.2}$$

$$G(\Omega_{t\eta}) - G(\Omega) = t[G'(\Omega), \eta] + o(t). \tag{2.3}$$

3. Optimality condition

Definition 3.1. We say that a domain $\Omega \in \mathcal{E}$ is a local minimizer of (1.1) (for the considered class of perturbations) if $\Omega \in \mathcal{E}_{ad}$ and, for all $\eta \in \mathcal{Q}(\Omega)$, there exists $t_0 > 0$ such that

$$\forall t \in [0, t_0],\ \Omega_{t\eta} \in \mathcal{E}_{ad} \Rightarrow J(\Omega) \leq J(\Omega_{t\eta}). \tag{3.1}$$

In particular, this condition will be satisfied if $\Omega \in \mathcal{E}_{ad}$ and, for all $z \in \mathcal{T}(\Omega)^N$, $N \in \mathbb{N}$, there exists $\rho_0 > 0$ such that

$$\forall \rho \in [0, \rho_0]^N,\ \Omega_{z,\rho} \in \mathcal{E}_{ad} \Rightarrow J(\Omega) \leq J(\Omega_{z,\rho}).$$

Definition 3.2. We say that a domain $\Omega \in \mathcal{E}_{ad}$ satisfies the constraint qualification condition if there exists $\eta \in \mathcal{Q}(\Omega)$ such that

$$G(\Omega) + [G'(\Omega), \eta] \in \mathrm{int}(-K).$$

Equivalently, this amounts to say that there exists $(z_1, ..., z_N) \in \mathcal{T}(\Omega)^N$, $N \in \mathbb{N}$, and $(\lambda_1, ..., \lambda_N) \in \mathbb{R}_+^N$ such that

$$G(\Omega) + \sum_{i=1}^{N} \lambda_i G'(\Omega)(z_i) \in \mathrm{int}(-K).$$

The following notations will be used in the sequel: Y' stands for the continuous dual space of Y, $\langle ., . \rangle_{Y',Y}$ is the corresponding duality pairing, and K^+ is the positive dual cone of K, *i.e.*,

$$K^+ = \{\mu \in Y', \langle \mu, y \rangle_{Y',Y} \geq 0\ \forall y \in K\}.$$

As K is convex and closed, we have the classical identity

$$K = \{y \in Y, \langle \mu, y \rangle_{Y',Y} \geq 0\ \forall \mu \in K^+\}. \tag{3.2}$$

The following result is proved in [11].

Theorem 3.3. *Let Ω be a local minimizer of (1.1) satisfying the constraint qualification condition. Then there exists $\mu \in K^+$ such that:*

$$J'(\Omega)(x) + \mu \circ G'(\Omega)(x) \geq 0 \qquad \forall x \in \mathcal{T}(\Omega), \tag{3.3}$$

$$\langle \mu, G(\Omega) \rangle_{Y',Y} = 0. \tag{3.4}$$

4. Lagrangian functional and saddle points

We define the Lagrangian functional $L : \mathcal{E} \times Y' \to \mathbb{R}$ in the classical way:

$$L(\Omega, \mu) = J(\Omega) + \langle \mu, G(\Omega) \rangle_{Y',Y}.$$

We refer *e.g.* to [17] for a detailed description of the Lagrangian formalism, and to [19] for its application in shape optimization.

Definition 4.1. We say that the pair $(\Omega, \mu) \in \mathcal{E} \times K^+$ is a local saddle point of L on $\mathcal{E} \times K^+$ if, for all $\eta \in \mathcal{Q}(\Omega)$, there exists $t_0 > 0$ such that

$$L(\Omega, \mu') \leq L(\Omega, \mu) \leq L(\Omega_{t\eta}, \mu) \qquad \forall (t, \mu') \in [0, t_0] \times K^+. \tag{4.1}$$

The following theorem shows a first relation between local minimizers and local saddle points.

Theorem 4.2. *Consider a pair $(\Omega, \mu) \in \mathcal{E}_{ad} \times K^+$ satisfying*

$$J'(\Omega)(x) + \mu \circ G'(\Omega)(x) > 0\ \forall x \in \mathcal{T}(\Omega),$$

$$\langle \mu, G(\Omega) \rangle_{Y',Y} = 0. \tag{4.2}$$

Then (Ω, μ) is a local saddle point of L on $\mathcal{E} \times K^+$.

Proof. (1) We begin by checking the first inequality in (4.1). In view of (4.2), we have that $L(\Omega, \mu) = J(\Omega)$. Thus, for all $\mu' \in Y'$,

$$L(\Omega, \mu') - L(\Omega, \mu) = \langle \mu', G(\Omega) \rangle_{Y',Y}.$$

Since $G(\Omega) \in -K$, this quantity is nonpositive whenever $\mu' \in K^+$.

(2) We turn to the second inequality. From the definition of the Lagrangian functional and Proposition 2.2 we derive:

$$\begin{aligned} L(\Omega_{t\eta},\mu) - L(\Omega,\mu) &= J(\Omega_{t\eta}) - J(\Omega) + \langle \mu, G(\Omega_{t\eta}) - G(\Omega)\rangle_{Y',Y} \\ &= t\left[J'(\Omega) + \mu \circ G'(\Omega), \eta\right] + o(t). \end{aligned}$$

With the assumptions made, $[J'(\Omega) + \mu \circ G'(\Omega), \eta] > 0$ as soon as η is not identically zero, which provides the desired inequality.

□

We now examine a converse of Theorem 4.2.

Theorem 4.3. *Let (Ω, μ) be a local saddle point of L on $\mathcal{E} \times K^+$. Then Ω is a local minimizer of (1.1). Moreover, (3.3) and (3.4) hold true.*

Proof. (1) By exploiting the first inequality in (4.1), we derive that

$$\langle \mu' - \mu, G(\Omega)\rangle_{Y',Y} \leq 0 \ \forall \mu' \in K^+.$$

Taking $\mu' = 0$ then $\mu' = 2\mu$ yields

$$\langle \mu, G(\Omega)\rangle_{Y',Y} = 0.$$

Therefore we have

$$\langle \mu', G(\Omega)\rangle_{Y',Y} \leq 0 \ \forall \mu' \in K^+.$$

By (3.2), this entails $G(\Omega) \in -K$, *i.e.*, $\Omega \in \mathcal{E}_{ad}$.

(2) Consider a perturbed domain $\Omega_{t\eta} \in \mathcal{E}_{ad}$. We have

$$\langle \mu, G(\Omega_{t\eta}) - G(\Omega)\rangle_{Y',Y} = \langle \mu, G(\Omega_{t\eta})\rangle_{Y',Y} \leq 0,$$

because $\mu \in K^+$ and $G(\Omega_{t\eta}) \in -K$. Therefore,

$$J(\Omega_{t\eta}) - J(\Omega) \geq L(\Omega_{t\eta}, \mu) - L(\Omega, \mu).$$

According to the second inequality in (4.1), the right hand side is nonnegative provided that t is sufficiently small. We conclude that Ω is a local minimizer of (1.1).

(3) It remains to prove (3.3). To do so, we take an arbitrary perturbation $\eta \in \mathcal{Q}(\Omega)$. From the second inequality in (4.1) together with (2.2) and (2.3), it comes

$$t[J'(\Omega) + \mu \circ G'(\Omega), \eta] + o(t) \geq 0$$

for all t sufficiently small. Dividing by $t > 0$ and passing to the limit when t goes to zero completes the proof.

□

5. Augmented Lagrangian

The augmented Lagrangian can be introduced in different ways. Here we partly follow the presentation of [18], with adaptation to our context. We assume that Y is a Hilbert space and we identify Y' with Y and the duality pairing $\langle ., . \rangle_{Y',Y}$ with the scalar product of Y. Given a positive parameter b, we define the augmented Lagrangian functional $L_b : \mathcal{E} \times Y' \to \mathbb{R}$ by:

$$L_b(\Omega, \mu) = J(\Omega) + \zeta_b(G(\Omega), \mu)$$

where, for all $y \in Y$, $\zeta_b(y, .)$ is the concave Moreau-Yosida transform of $\langle y, . \rangle$ with constant $1/b$ over K^+, *i.e.*,

$$\zeta_b(y, \mu) = \sup_{\mu' \in K^+} \left(\langle y, \mu' \rangle - \frac{1}{2b} \|\mu - \mu'\|^2 \right). \tag{5.1}$$

We denote by P_{K+} the projection operator from Y onto the closed convex set K^+, and by d_{K^+} the Euclidean distance operator to K^+. A proof of the following lemma can be found in [15].

Lemma 5.1. *The function $v : y \in Y \mapsto \dfrac{1}{2} d_{K^+}(y)^2$ is continuously differentiable with gradient*

$$\nabla v(y) = y - P_{K^+}(y).$$

The following theorem provides explicit expressions of the function ζ_b along with its derivatives. Although these results are classical, we briefly give a proof for completeness.

Theorem 5.2. (1) *At all pair $(y,\mu)\in Y\times Y$ the function ζ_b admits the expressions*

$$\zeta_b(y,\mu) = \frac{1}{2b}\left(\|P_{K^+}(\mu+by)\|^2-\|\mu\|^2\right) \tag{5.2}$$

$$= \langle\mu,y\rangle+\frac{b}{2}\|y\|^2-\frac{1}{2b}d_{K^+}(\mu+by)^2. \tag{5.3}$$

(2) *For all $\mu\in Y$, the function $\zeta_b(.,\mu)$ is differentiable on Y with gradient*

$$\nabla_y\zeta_b(y,\mu)=P_{K^+}(\mu+by). \tag{5.4}$$

For all $y\in Y$, the function $\zeta_b(y,.)$ is differentiable on Y with gradient

$$\nabla_\mu\zeta_b(y,\mu)=\frac{1}{b}\left(P_{K^+}(\mu+by)-\mu\right). \tag{5.5}$$

Proof. (1) It comes by standard arguments that the supremum in (5.1) is attained at some unique point $\hat\mu\in K^+$, and that a necessary first order optimality condition reads

$$\langle y+\frac{1}{b}(\mu-\hat\mu),\mu'-\hat\mu\rangle\le 0\ \forall\mu'\in K^+.$$

As $b>0$, this inequality can be equivalently rewritten as

$$\langle by+\mu-\hat\mu,\mu'-\hat\mu\rangle\le 0\ \forall\mu'\in K^+.$$

Hence $\hat\mu=P_{K^+}(by+\mu)$. Reporting this expression into (5.1) results in

$$\begin{aligned}\zeta_b(y,\mu) &= \langle y,P_{K^+}(by+\mu)\rangle-\frac{1}{2b}\|\mu-P_{K^+}(by+\mu)\|^2\\ &= \langle y+\frac{1}{b}\mu,P_{K^+}(by+\mu)\rangle-\frac{1}{2b}\|\mu\|^2-\frac{1}{2b}\|P_{K^+}(by+\mu)\|^2.\end{aligned}$$

Since K^+ is a cone, the first term is equal to twice the latter. Formula (5.2) follows. For every $x\in Y$, we have

$$d_{K^+}(x)^2=\|P_{K^+}(x)-x\|^2=\|P_{K^+}(x)\|^2+\|x\|^2-2\langle P_{K^+}(x),x\rangle=-\|P_{K^+}(x)\|^2+\|x\|^2,$$

where the latter equality stems again from the cone property. The above relation provides straightforwardly the equality between (5.2) and (5.3).

(2) Starting from (5.3) and differentiating with respect to y and μ by using Lemma 5.1 yields (5.4) and (5.5), respectively.

□

The following properties are also classical, apart from the fact that the Moreau-Yosida regularization is here computed in a cone. Therefore we provide a short proof.

Lemma 5.3. (1) *For all $(y,\mu)\in Y\times K^+$, we have*

$$\langle y,\mu\rangle\le\zeta_b(y,\mu).$$

(2) *For all $y\in Y$, we have*

$$\sup_{\mu\in K^+}\langle y,\mu\rangle=\sup_{\mu\in Y}\zeta_b(y,\mu).$$

(3) *For all $y\in -K$, the above suprema are attained and*

$$\operatorname*{argmax}_{\mu\in K^+}\langle y,\mu\rangle=\operatorname*{argmax}_{\mu\in Y}\zeta_b(y,\mu).$$

Proof. (1) Taking $\mu'=\mu$ in (5.1) provides straightforwardly the first inequality.

(2) The second inequality is obtained by writing

$$\begin{aligned}\sup_{\mu\in Y}\zeta_b(y,\mu) &= \sup_{\mu\in Y}\sup_{\mu'\in K^+}\left(\langle y,\mu'\rangle-\frac{1}{2b}\|\mu-\mu'\|^2\right)\\ &= \sup_{\mu'\in K^+}\sup_{\mu\in Y}\left(\langle y,\mu'\rangle-\frac{1}{2b}\|\mu-\mu'\|^2\right)\\ &= \sup_{\mu'\in K^+}\langle y,\mu'\rangle.\end{aligned}$$

(3) As $y \in -K$, $\langle y, \mu\rangle \leq 0$ for all $\mu \in K^+$. Hence $\sup_{\mu\in K^+}\langle y, \mu\rangle$ is attained at $\mu = 0$. Consider some $\hat{\mu} \in \operatorname{argmax}_{\mu\in K^+}\langle y, \mu\rangle$. Then $\langle y, \hat{\mu}\rangle = \sup_{\mu\in K^+}\langle y, \mu\rangle = \sup_{\mu\in Y}\zeta_b(y, \mu) \geq \zeta_b(y, \hat{\mu}) \geq \langle y, \hat{\mu}\rangle$. Therefore all the inequalities are equalities, in particular $\sup_{\mu\in Y}\zeta_b(y, \mu) = \zeta_b(y, \hat{\mu})$. This entails $\hat{\mu} \in \operatorname{argmax}_{\mu\in Y}\zeta_b(y, \mu)$. Conversely, consider $\hat{\mu} \in \operatorname{argmax}_{\mu\in Y}\zeta_b(y, \mu)$. Then $\zeta_b(y, \hat{\mu}) = \sup_{\mu\in Y}\zeta_b(y, \mu) = \sup_{\mu\in K^+}\langle y, \mu\rangle = 0$. Yet, the supremum in (5.1) is attained: there exists $\mu' \in K^+$ such that

$$\langle y, \mu'\rangle - \frac{1}{2b}\|\hat{\mu} - \mu'\|^2 = \zeta_b(y, \hat{\mu}) = 0.$$

Both terms in the left hand side are nonpositive, hence $\hat{\mu} = \mu' \in K^+$ and $\langle y, \hat{\mu}\rangle = 0 = \sup_{\mu\in K^+}\langle y, \mu\rangle$. Therefore $\hat{\mu} \in \operatorname{argmax}_{\mu\in K^+}\langle y, \mu\rangle$.

□

We are now in position to prove the main theorem of this section.

Theorem 5.4. (1) *If (Ω, μ) is a local saddle point of L on $\mathcal{E} \times K^+$, then (Ω, μ) is a local saddle point of L_b on $\mathcal{E} \times Y$ and $L_b(\Omega, \mu) = L(\Omega, \mu)$.*

(2) *If (Ω, μ) is a local saddle point of L_b on $\mathcal{E} \times Y$, then $(\Omega, \mu) \in \mathcal{E}_{ad} \times K^+$ and (3.3)-(3.4) are satisfied. Moreover, $L_b(\Omega, \mu) = L(\Omega, \mu)$.*

Proof. (1) We assume that (Ω, μ) is a local saddle point of L on $\mathcal{E} \times K^+$. According to Theorem 4.3, we have $G(\Omega) \in -K$. Next, the function $\mu' \in K^+ \mapsto L(\Omega, \mu')$ attains its maximum at μ. Hence, by Lemma 5.3, the function $\mu' \in Y \mapsto L_b(\Omega, \mu')$ attains its maximum at μ as well and

$$L_b(\Omega, \mu) = L(\Omega, \mu). \tag{5.6}$$

In other words,

$$L_b(\Omega, \mu') \leq L_b(\Omega, \mu)\ \forall \mu' \in Y.$$

We now turn to the second inequality. Given a perturbation $\eta \in \mathcal{Q}(\Omega)$ there exists $t_0 > 0$ such that $L(\Omega, \mu) \leq L(\Omega_{t\eta}, \mu)$ for all $t \leq t_0$. Lemma 5.3 implies that $L(\Omega_{t\eta}, \mu) \leq L_b(\Omega_{t\eta}, \mu)$, which, together with (5.6), yields

$$L_b(\Omega, \mu) \leq L_b(\Omega_{t\eta}, \mu)\ \forall t \leq t_0.$$

(2) We assume now that (Ω, μ) is a local saddle point of L_b on $\mathcal{E} \times Y$. As L_b is differentiable with respect to μ, we have $\nabla_\mu L_b(\Omega, \mu) = 0$. Thus, $\nabla_\mu \zeta_b(G(\Omega), \mu) = 0$. Then, using (5.5), it comes

$$P_{K^+}(\mu + bG(\Omega)) = \mu. \tag{5.7}$$

We deduce that $\mu \in K^+$. Moreover, μ satisfies

$$\langle(\mu + bG(\Omega)) - \mu, y - \mu\rangle \leq 0\ \forall y \in K^+. \tag{5.8}$$

Taking $y = 0$ then $y = 2\mu$ entails $\langle G(\Omega), \mu\rangle = 0$. Consequently, (5.8) reduces to

$$\langle G(\Omega), y\rangle \leq 0\ \forall y \in K^+,$$

which implies that $G(\Omega) \in -K$. Next, arguing that the function $\mu' \in Y \mapsto \zeta_b(G(\Omega), \mu')$ attains its maximum at μ, Lemma 5.3 yields

$$L(\Omega, \mu') \leq L(\Omega, \mu) = L_b(\Omega, \mu)\ \forall \mu' \in K^+.$$

Using (5.4) and (5.7), it comes $\nabla_y \zeta_b(G(\Omega), \mu) = \mu$. From the second inequality in (4.1) for L_b we obtain that, for any perturbation $\eta \in \mathcal{Q}(\Omega)$ and any $t \geq 0$ sufficiently small,

$$J(\Omega_{t\eta}) - J(\Omega) + \zeta_b(G(\Omega_{t\eta}), \mu) - \zeta_b(G(\Omega), \mu) \geq 0.$$

Next, using the differentiability of ζ_b it comes

$$J(\Omega_{t\eta}) - J(\Omega) + \langle\nabla_y \zeta_b(G(\Omega), \mu), G(\Omega_{t\eta}) - G(\Omega)\rangle + o(\|G(\Omega_{t\eta}) - G(\Omega)\|) \geq 0. \tag{5.9}$$

It stems from (2.3) that $\|G(\Omega_{t\eta}) - G(\Omega)\| = O(t)$. Then, taking into account the equality $\nabla_y \zeta_b(G(\Omega), \mu) = \mu$, (5.9) yields

$$\lim_{t\to 0} \frac{J(\Omega_{t\eta}) - J(\Omega) + \langle\mu, G(\Omega_{t\eta}) - G(\Omega)\rangle}{t} \geq 0.$$

Thus Proposition 2.2 leads to $[J'(\Omega) + \mu \circ G'(\Omega), \eta] \geq 0$. Since this inequality holds for every $\eta \in \mathcal{Q}$, we deduce that $J'(\Omega)(x) + \mu \circ G'(\Omega)(x) \geq 0$ for all $x \in \mathcal{T}(\Omega)$.

□

We shall now synthesize the obtained results. Gathering Theorems 3.3, 4.2, 4.3 and 5.4 leads to the following relations.

Theorem 5.5. *Consider a domain $\Omega \in \mathcal{E}$ satisfying*

$$J'(\Omega)(x) + \mu \circ G'(\Omega)(x) \neq 0 \ \forall x \in \mathcal{T}(\Omega). \tag{5.10}$$

The following statements are equivalent (for the third one it is required that Y is a Hilbert space).

1. *The domain Ω is a local minimizer of (1.1). Moreover, there exists a Lagrange multiplier $\mu \in K^+$ such that (3.3)-(3.4) hold true (which is automatically satisfied if the constraint qualification condition is fulfilled).*
2. *The pair (Ω, μ) is a local saddle point of the Lagrangian L on $\mathcal{E} \times K^+$.*
3. *The pair (Ω, μ) is a local saddle point of the augmented Lagrangian L_b on $\mathcal{E} \times Y$.*

We point out that the condition (5.10) is in practice rather mild. It can be simply bypassed by removing the vanishing set from $\mathcal{T}(\Omega)$, which amounts to restrict the class of perturbations in the definition of local optimal domains.

6. Algorithm

In view of Theorem 5.5, the search for a local minimizer of (1.1) is replaced by the search for a local saddle point of the Lagrangian (possibly augmented). In the spirit of the Uzawa algorithm, we will alternatively perform a minimization with respect to the domain, and make a gradient step in the dual direction. Since in the numerical applications the space of constraints Y is, after possible discretization, of finite dimension, we assume in this section that Y is a Hilbert space and we identify Y with Y'. We recall that P_{K+} denotes the projection operator from Y onto K^+. In the case of inequality constraints, this operator consists in taking the positive part of a vector, which is particularly easy to implement.

Algorithm 1 (ordinary Lagrangian)

1. Choose $\Omega_0 \in \mathcal{E}$ and $\mu_0 \in K^+$. Set $k = 0$. Fix $\tau > 0$ and $\varepsilon_{stop} > 0$.
2. Starting from Ω_k, find a local minimizer Ω_{k+1} of the problem
$$\min_{\Omega \in \mathcal{E}} L(\Omega, \mu_k).$$
3. Set $\mu_{k+1} = P_{K^+}(\mu_k + \tau G(\Omega_{k+1}))$.
4. If $\|\mu_{k+1} - \mu_k\| \leq \varepsilon_{stop}$ then stop else increment $k \leftarrow k+1$ and goto (2).

Algorithm 2 (augmented Lagrangian)

1. Choose $\Omega_0 \in \mathcal{E}$ and $\mu_0 \in Y$. Set $k = 0$. Fix $b > 0$, $\tau > 0$ and $\varepsilon_{stop} > 0$.
2. Starting from Ω_k, find a local minimizer Ω_{k+1} of the problem
$$\min_{\Omega \in \mathcal{E}} L_b(\Omega, \mu_k). \tag{6.1}$$
3. Set $\mu_{k+1} = \mu_k + \dfrac{\tau}{b}[P_{K^+}(\mu_k + bG(\Omega_{k+1})) - \mu_k]$.
4. If $\|\mu_{k+1} - \mu_k\| \leq \varepsilon_{stop}$ then stop else increment $k \leftarrow k+1$ and goto (2).

It turns out that, like in differentiable optimization, the second algorithm is generally much faster. It has another advantage: the stepsize τ, rather arbitrary in the first algorithm, is usually chosen equal to b (see, *e.g.*, [15]). However, choosing an adequate value for b may require a few tests, because taking it too large makes Problem (6.1) ill-conditioned. This phenomenon is generally clearly observable after a few iterations.

In order to solve the unconstrained minimization problem for the (augmented) Lagrangian (step 2 in both algorithms), we use the algorithm described in [10]. It roughly works as follows. Every domain Ω is represented by a function $\psi : D \to \mathbb{R}$ such that $\Omega(\psi) = \{x \in D, \psi(x) < 0\}$ and $D \setminus \overline{\Omega(\psi)} = \{x \in D, \psi(x) > 0\}$. The algorithm is based on the solving of the sufficient optimality condition at μ fixed:

$$\tilde{g}(\Omega(\psi)) \sim \psi,$$

with

$$\tilde{g}(\Omega)(x) = \begin{cases} -[J'(\Omega)(x) + \mu \circ G'(\Omega)(x)] & \text{if} \quad x \in \Omega, \\ J'(\Omega)(x) + \mu \circ G'(\Omega)(x) & \text{if} \quad x \in D \setminus \overline{\Omega}, \end{cases}$$

$$\psi_1 \sim \psi_2 \Longleftrightarrow \exists \alpha > 0, \psi_1 = \alpha \psi_2.$$

A fixed point type method on the unit sphere $\{\psi \in L^2(D), \|\psi\|_{L^2(D)} = 1\}$ is applied. At convergence, the mesh may be automatically locally refined by means of a posteriori error estimates if the above optimality condition is not satisfactorily met, namely the angle between the level-set function ψ and the signed topological derivative $\tilde{g}(\Omega(\psi))$ is greater than 5 degrees.

In the next two sections, we consider structural optimization problems with constraints on the compliance and eigenfrequencies. We show results obtained by using the augmented Lagrangian only. We do not attempt to illustrate the superiority of this latter on the ordinary Lagrangian. We justify this choice by two reasons. Firstly, topology optimization problems are usually severely ill-posed, in the sense that they possess many local minima and no global minimum. Therefore two algorithms often lead to two different solutions. Secondly, we have observed in our context the well-known advantages of the augmented Lagrangian, namely it permits a smooth convergence of the Lagrange multiplier for a larger stepsize.

In the subsequent examples, $\mathcal{E}$ contains all subsets of D, and $\Omega_0 = D$ (full domain initialization).

7. Numerical examples in structural optimization with a constraint on the first eigenfrequency

7.1. **Problem statement.** We consider the following optimum design problem in plane stress linearized elasticity: minimize the area of the domain with an upper bound on the compliance and a lower bound on the first eigenfrequency. We assume that the boundary ∂D of the computational domain D consists of three disjoint parts Γ_F, Γ_0 and Γ_D, with $\text{meas}(\Gamma_D) > 0$. Given a load $F \in H^{-1/2}(\Gamma_F)$, the state equations for the displacement field u_Ω read:

$$\left\{ \begin{array}{rcl} -\text{div } \sigma_\Omega(u_\Omega) = 0 & \text{in} & D, \\ \sigma_\Omega(u_\Omega)n = F & \text{on} & \Gamma_F, \\ \sigma_\Omega(u_\Omega)n = 0 & \text{on} & \Gamma_0, \\ u_\Omega = 0 & \text{on} & \Gamma_D. \end{array} \right.$$

Here, $\sigma_\Omega(u)$ stands for the stress tensor, which depends linearly on the spatial derivatives of the displacement u through the Hooke law. The Young modulus is chosen equal to 1 in Ω and $\varepsilon_s = 10^{-3}$ in $D \setminus \overline{\Omega}$. The Poisson ratio is equal to 0.3 everywhere in D. The vector n is the outward unit normal to ∂D. The compliance is computed by

$$C_\Omega = \int_{\Gamma_F} F.u_\Omega ds,$$

the integral symbol being used for readability to denote the duality pairing between $H^{-1/2}(\Gamma_F)$ and $H^{1/2}(\Gamma_F)$. The first eigenfrequency Λ_Ω and the associated eigenfunction v_Ω solve:

$$\left\{ \begin{array}{rcl} -\text{div } \sigma_\Omega(v_\Omega) = \Lambda_\Omega \gamma_\Omega v_\Omega & \text{in} & D, \\ \sigma_\Omega(v_\Omega)n = 0 & \text{on} & \Gamma_F, \\ \sigma_\Omega(v_\Omega)n = 0 & \text{on} & \Gamma_0, \\ v_\Omega = 0 & \text{on} & \Gamma_D. \end{array} \right.$$

Following [4], the density γ_Ω is taken equal to 1 in Ω and $\varepsilon_d = 10^{-6}$ in $D \setminus \overline{\Omega}$ in order to avoid undesirable eigenmodes localized in the weak phase. Given two positive numbers C_{max} and Λ_{min}, we define two constraint functionals:

$$G_1(\Omega) = C_\Omega - C_{max}, \qquad G_2(\Omega) = \Lambda_{min} - \Lambda_\Omega.$$

Thus the problem under investigation can be written

$$\min_{\Omega \in \mathcal{E}} J(\Omega) = |\Omega| \quad \text{subject to} \quad (G_1(\Omega), G_2(\Omega)) \in \mathbb{R}_- \times \mathbb{R}_-.$$

We do not impose any restriction on the topology perturbations, *i.e.*, $\mathcal{T}(\Omega) = D \setminus \partial\Omega$. The topological sensitivity of the objective functional is obvious, namely:

$$f(\rho) = \pi \rho^2, \qquad J'(\Omega)(x) = \left\{ \begin{array}{rcl} -1 & \text{if} & x \in \Omega, \\ 1 & \text{if} & x \in D \setminus \overline{\Omega}. \end{array} \right.$$

For the compliance, we have:

$$C_{\Omega_{z,\rho}} - C_\Omega = \sum_{i=1}^{N} \pi \rho_i^2 C'_\Omega(u_\Omega)(z_i) + o(\rho^2), \tag{7.1}$$

with

$$C'_\Omega(u_\Omega) = \begin{cases} \frac{1-\varepsilon_s}{\kappa\varepsilon_s+1}\frac{\kappa+1}{2}\left[2\sigma_\Omega(u_\Omega) : e(u_\Omega) + \frac{(\varepsilon_s-1)(\kappa-2)}{\kappa+2\varepsilon_s-1}\mathrm{tr}\sigma_\Omega(u_\Omega)\mathrm{tr}e(u_\Omega)\right] & \text{in} \quad \Omega, \\ -\frac{1-\varepsilon_s}{\kappa+\varepsilon_s}\frac{\kappa+1}{2}\left[2\sigma_\Omega(u_\Omega) : e(u_\Omega) + \frac{(1-\varepsilon_s)(\kappa-2)}{\kappa\varepsilon_s+2-\varepsilon_s}\mathrm{tr}\sigma_\Omega(u_\Omega)\mathrm{tr}e(u_\Omega)\right] & \text{in} \quad D\setminus\overline{\Omega}. \end{cases}$$

In the above expression,

$$\kappa = \frac{\lambda_L + 3\mu_L}{\lambda_L + \mu_L}$$

where λ_L, μ_L denote the Lamé coefficients of the material, and e stands for the strain tensor. This expression is established in [8] for a single inclusion. The extension to multiple inclusions can be derived by arguing like in [11] (see also [30, 12] for the creation of holes). The topological derivative for simple eigenvalues of the Laplacian is obtained in [7] (see [27, 28] for the generalization to multiple eigenvalues and other types of singular domain perturbations). The polarization tensor formalism enables straightforward extensions of this result to other linear elliptic operators. In the linear elasticity case, using the polarization tensor given in [6], we obtain

$$\Lambda_{\Omega_{z,\rho}} - \Lambda_\Omega = \sum_{i=1}^{N} \pi \rho_i^2 \Lambda'_\Omega(v_\Omega)(z_i) + o(\rho^2), \tag{7.2}$$

with

$$\Lambda'_\Omega(v_\Omega) = \frac{-C'_\Omega(v_\Omega) - \Lambda_\Omega s(1-\varepsilon_d)|v_\Omega|^2}{\int_D \gamma_\Omega |v_\Omega|^2},$$

$$s(x) = \begin{cases} -1 & \text{if} \quad x \in \Omega, \\ 1 & \text{if} \quad x \in D\setminus\overline{\Omega}. \end{cases}$$

7.2. **Mast.** The first example is the classical mast problem. The geometry and the boundary conditions are sketched on Figure 1 (left). To begin with, we only consider a constraint on the compliance, which has to be less than 80. We choose the augmentation parameter $b = 5.10^{-3}$. We obtain the domain depicted on Figure 1 (middle), after a computation using $268s$ of CPU time on a PC with 2.4 GHz processor. The compliance of this domain is $C_\Omega = 80.3$ and the first eigenfrequency is $\Lambda_\Omega = 2.1\ 10^{-4}$. Convergence histories are provided on Figure 2, in which the horizontal axis represents the number of iterations, an iteration corresponding to one step in the solving of (6.1). Note that this computer time contains a large part of eigenvalue analysis, even if the eigenvalues are not taken into account in this computation.

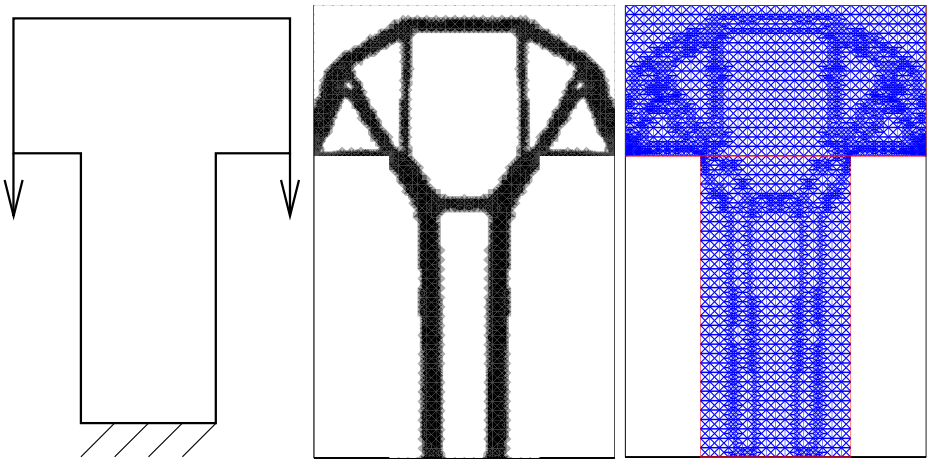

FIGURE 1. Mast: boundary conditions (left), obtained design with compliance constraint (middle), and mesh (4891 nodes, right).

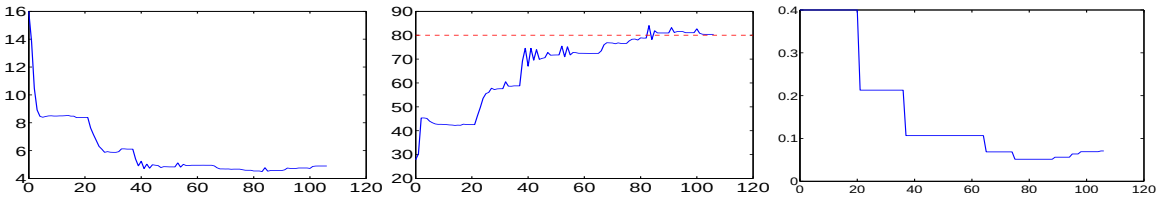

FIGURE 2. Mast with compliance constraint: convergence histories for the area (left), the compliance (middle) and the Lagrange multiplier (right).

We now consider the additional constraint $\Lambda_\Omega \geq 2.10^{-3}$. We use the augmentation parameters $b_C = 5.10^{-3}$ for the compliance and $b_\Lambda = 10^6$ for the first eigenfrequency. Constraints of different natures and different scales should indeed be handled with different augmentation parameters. The theory developed before can be easily extended to this situation. We obtain a domain such that $C_\Omega = 80.3$ and $\Lambda_\Omega = 1.98\ 10^{-3}$ (see Figures 3 and 4, $389s$ of CPU time). Note that the first eigenfrequency remains simple throughout the optimization process. Clearly, this mast is much more robust than the previous one with respect to bending around the vertical axis of symmetry.

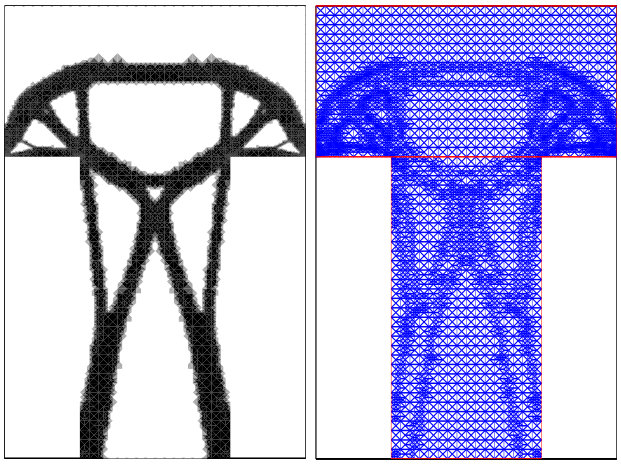

FIGURE 3. Mast with compliance and eigenfrequency constraints and mesh (5919 nodes).

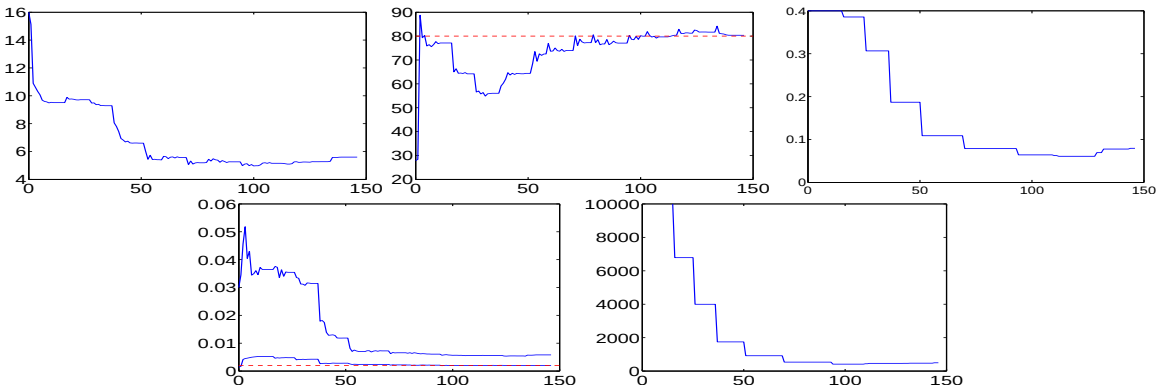

FIGURE 4. Mast with compliance and eigenfrequency constraints. Top: convergence histories for the area, the compliance and the Lagrange multiplier for the compliance. Bottom: first two eigenfrequencies and Lagrange multiplier for the first eigenfrequency.

7.3. **Long cantilever.** We consider now the long cantilever problem (see Figure 5, left). The compliance must be less than 100 and the first eigenfrequency more than 0.12. We use the augmentation parameters $b_C = 5.10^{-4}$ and $b_\Lambda = 200$. We obtain a structure with compliance $C_\Omega = 100.1$ and first eigenfrequency $\Lambda_\Omega = 0.1196$ after a computation of $323s$ (see Figures 5 and 6).

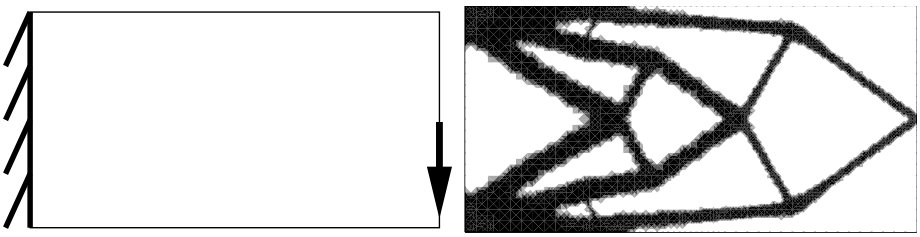

FIGURE 5. Cantilever with compliance and eigenfrequency constraints.

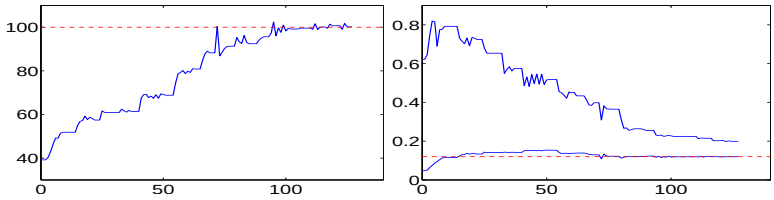

FIGURE 6. Cantilever: convergence histories for the compliance (left) and the first two eigenfrequencies (right).

8. Numerical examples in structural optimization with multiple loads

8.1. **General setting.** We consider again a computational domain D occupied by a two phase elastic material. The geometrical requirements and the elastic properties are the same as before. Now, the structure is subject to a family of loads $(F_\xi)_{\xi\in I}$, where the index set I is a compact subset of $\mathbb{R}$. Denoting by $u_{\Omega,\xi}$ the displacement field associated with the domain Ω and the load F_ξ, the governing equations read:

$$\left\{\begin{array}{rcl} -\text{div }\sigma_\Omega(u_{\Omega,\xi}) = 0 & \text{in} & D, \\ \sigma_\Omega(u_{\Omega,\xi})n = F_\xi & \text{on} & \Gamma_F, \\ \sigma_\Omega(u_{\Omega,\xi})n = 0 & \text{on} & \Gamma_0, \\ u_{\Omega,\xi} = 0 & \text{on} & \Gamma_D. \end{array}\right.$$

The objective functional to be minimized is again the volume $J(\Omega) = |\Omega|$. The constraint is an upper bound C_{max} on the compliance corresponding to each load. Therefore the function G is defined by

$$\begin{array}{rccc} G(\Omega): & I & \to & \mathbb{R} \\ & \xi & \mapsto & C_\Omega(\xi) - C_{max} \end{array}$$

with the compliance

$$C_\Omega(\xi) = \int_{\Gamma_F} F_\xi . u_{\Omega,\xi} ds.$$

We assume that the mapping

$$\begin{array}{ccc} I & \to & H^{-1/2}(\Gamma_F) \\ \xi & \mapsto & F_\xi \end{array}$$

is continuous, which will hold true in the presented examples. It follows by elliptic regularity that the composite mapping $G(\Omega) : I \to \mathbb{R}$ is also continuous. Therefore the relevant sets are $Y = \mathcal{C}(I)$ and $K = \{y \in Y, y(\xi) \geq 0\ \forall \xi \in I\}$. Then we have $Y' = \mathcal{M}(I)$ and $K^+ = \mathcal{M}^+(I)$, the set of Radon measures and positive Radon measures on I, respectively. As in the previous example, we have the following topological sensitivity:

$$\forall \xi \in I,\ C_{\Omega_{z,\rho}}(\xi) - C_\Omega(\xi) = \sum_{i=1}^{N} \pi \rho_i^2 C'_\Omega(\xi)(z_i) + o(\rho^2), \tag{8.1}$$

with

$$C'_\Omega(\xi) = \begin{cases} \frac{1-\varepsilon_s}{\kappa\varepsilon_s+1}\frac{\kappa+1}{2}\left[2\sigma(u_{\Omega,\xi}) : e(u_{\Omega,\xi}) + \frac{(\varepsilon_s-1)(\kappa-2)}{\kappa+2\varepsilon_s-1}\mathrm{tr}\sigma(u_{\Omega,\xi})\mathrm{tr}e(u_{\Omega,\xi})\right] & \text{in} \quad \Omega, \\ -\frac{1-\varepsilon_s}{\kappa+\varepsilon_s}\frac{\kappa+1}{2}\left[2\sigma(u_{\Omega,\xi}) : e(u_{\Omega,\xi}) + \frac{(1-\varepsilon_s)(\kappa-2)}{\kappa\varepsilon_s+2-\varepsilon_s}\mathrm{tr}\sigma(u_{\Omega,\xi})\mathrm{tr}e(u_{\Omega,\xi})\right] & \text{in} \quad D\setminus\overline{\Omega}. \end{cases}$$

By arguing like in [11], we obtain that the remainder "$o(\rho^2)$" is uniform with respect to ξ on I. We deduce that (2.1) holds true with $f(\rho) = \pi\rho^2$ and $G'(\Omega) : \xi \mapsto C'(\Omega)(\xi)$. Thus Assumption 2.1 is fulfilled.

8.2. **Discretization of the set of constraints.** We select a finite number of points $\xi_1, ..., \xi_n \in I$ for which the constraint will be observed. Hence the discretized constraint reads $G(\Omega)(\xi) \leq 0$ for all $\xi \in I_n := \{\xi_1, ..., \xi_n\}$. The general framework applies by substituting $Y_n = \mathbb{R}^n$ for Y and $K_n = \mathbb{R}^n_+$ for K. In the subsequent examples, we choose a regular discretization of I, hence we use the canonical scalar product on $\mathbb{R}^n$. Identifying Y'_n with Y_n, we have $K_n^+ = \mathbb{R}^n_+$.

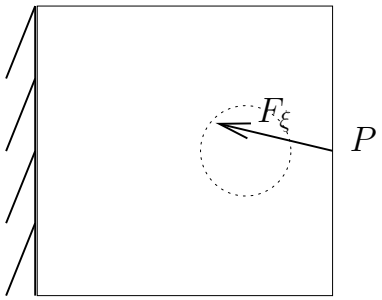

FIGURE 7. Boundary conditions for the beam problem.

8.3. **Beam.** We consider the problem depicted in Figure 7. The working domain is the square $D = [0,1] \times [0,1]$. The family of loads is indexed by the angle $\xi \in I = [0, 2\pi]$. For any $\xi \in I$, F_ξ is a pointwise force applied at the middle of the right edge, given by

$$F_\xi = \left[\begin{pmatrix} -1 \\ 0 \end{pmatrix} + m \begin{pmatrix} \cos\xi \\ \sin\xi \end{pmatrix}\right] \delta_P.$$

In this expression, m is a nonnegative parameter. For the problem with discretized state equation, δ_P is the discrete Dirac function at the point P. At the continuous level, the correspondence can be obtained by taking δ_P as the characteristic function of a small neighborhood of P on ∂D.

We consider several cases, depending on the value of m. In every case, the compliance threshold is $C_{max} = 10$, the initial mesh is regular and consists of 2113 nodes. We use the augmented Lagrangian with $b = 10^{-4}$. The initial Lagrange multiplier is constant and equal to $\mu_0 = 0.2$.

(1) The case where $m = 0$ is special since there is only one constraint. The result of the computation entirely performed on the initial regular mesh is shown in Figures 8 (left) and 9. At convergence, the compliance is equal to 10.06. Then the mesh is refined and the optimization is continued. This procedure is repeated several times. The final mesh consists of 3145 nodes. The compliance is equal to 9.84.
(2) For $m > 0$, the set of constraints is discretized with the help of $n = 64$ points. The results obtained for $m = 0.1$, $m = 0.2$ and $m = 0.3$ are depicted on Figures 10,11,12,13 and 14. For $m = 0.1$, the CPU time used is of 1097s. For $m = 0.2$, we present a first result obtained by a computation of 1080s. As the constraint is slightly violated, the procedure is continued (2535s for the whole computation). This shows that the computer time can be significantly reduced by the use of a safety factor on the constraint. In the last case ($m = 0.3$), the parameter b has been chosen equal to 10^{-2} in order to speed up the convergence (785s).

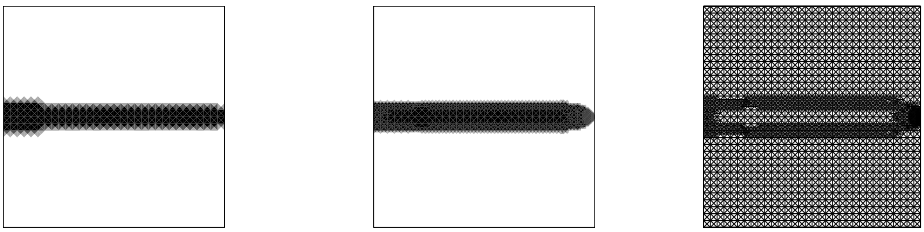

FIGURE 8. Beam with $m = 0$: design obtained on the regular mesh (left) and on the refined mesh (middle) with the corresponding mesh (right).

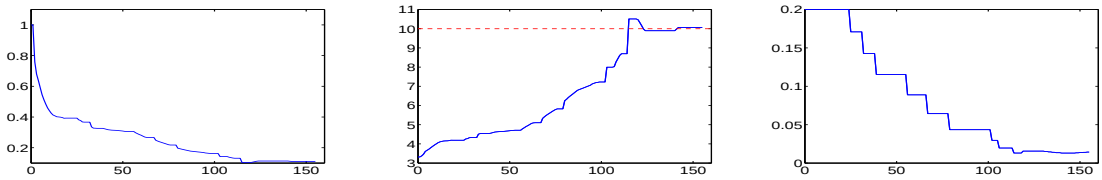

FIGURE 9. Beam with $m = 0$. Convergence histories for the area (left), the compliance (middle) and the Lagrange multiplier (right) before mesh refinement.

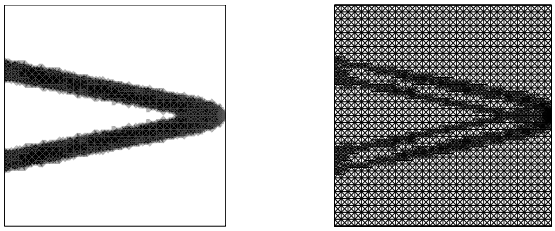

FIGURE 10. Beam with $m = 0.1$: design (left) and mesh (right, 3413 nodes).

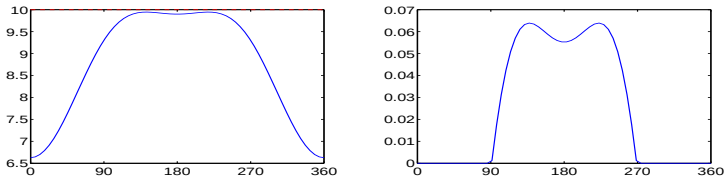

FIGURE 11. Beam with $m = 0.1$: compliance distribution (left) and Lagrange multiplier (right). The horizontal axis represents the angle ξ expressed in degrees.

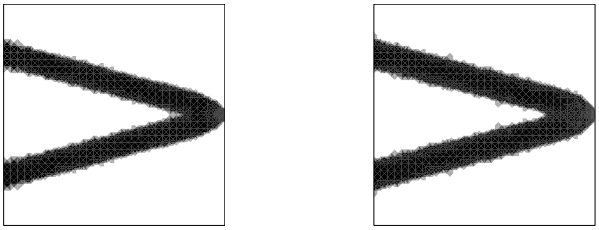

FIGURE 12. Beam with $m = 0.2$. Intermediate result (left) and final result (right).

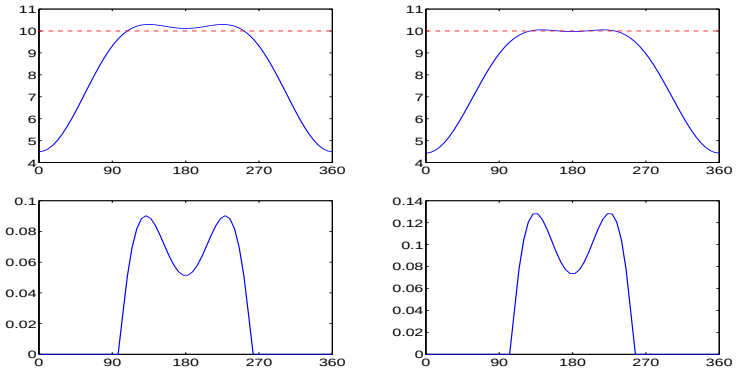

FIGURE 13. Beam with $m = 0.2$: compliance distribution and Lagrange multiplier for the intermediate result (left) and for the final result (right).

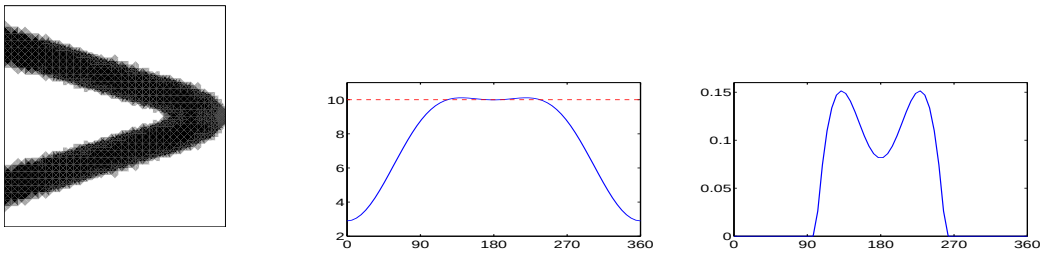

FIGURE 14. Beam with $m = 0.3$: design (left), compliance distribution (middle) and Lagrange multiplier (right).

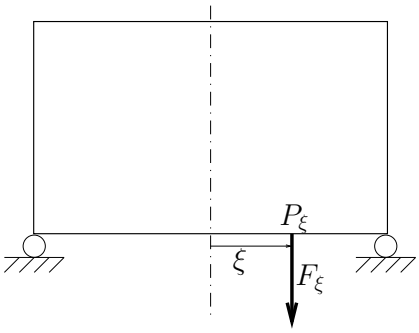

FIGURE 15. Boundary conditions for the bridge problem.

8.4. **Bridge.** The computational domain is the rectangle $D = [-1, 1] \times [0, 1.2]$ (see Figure 15). The loads consist of a family of pointwise forces $(F_\xi)_{\xi\in[-1,1]}$ applied at the bottom edge. They are given by

$$F_\xi = \begin{pmatrix} -1 \\ 0 \end{pmatrix} \delta_{P_\xi},$$

where P_ξ is the point of coordinates $(0, \xi)$. We apply the augmented Lagrangian algorithm with $b = 2.10^{-3}$ and the initial Lagrange multiplier $\mu_0 = 0.1$. The upper bound on the compliance is $C_{max} = 25$. The obtained result is shown on Figure 16 (1730s of CPU time).

REFERENCES

[1] G. Allaire. *Shape optimization by the homogenization method*, volume 146 of *Applied Mathematical Sciences*. Springer-Verlag, New York, 2002.

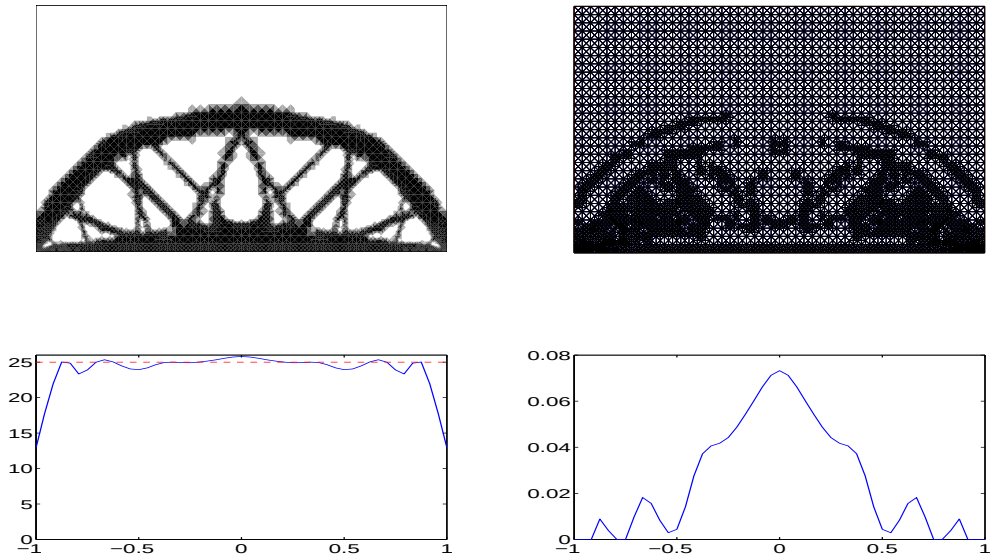

FIGURE 16. Bridge: obtained design (top left), final mesh (top right, 5771 nodes), compliance distribution (bottom left) and Lagrange multiplier (bottom right).

[2] G. Allaire. *Conception optimale de structures*, volume 58 of *Mathématiques & Applications (Berlin) [Mathematics & Applications]*. Springer-Verlag, Berlin, 2007. With the collaboration of Marc Schoenauer (INRIA) in the writing of Chapter 8.

[3] G. Allaire, F. de Gournay, F. Jouve, and A.-M. Toader. Structural optimization using topological and shape sensitivity via a level set method. *Control Cybern.*, 34:59–80, 2005.

[4] G. Allaire and F. Jouve. A level-set method for vibration and multiple loads structural optimization. *Comput. Methods Appl. Mech. Engrg.*, 194(30-33):3269–3290, 2005.

[5] G. Allaire, F. Jouve, and A.-M. Toader. Structural optimization using sensitivity analysis and a level-set method. *J. Comput. Phys.*, 194(1):363–393, 2004.

[6] H. Ammari and H. Kang. *Reconstruction of small inhomogeneities from boundary measurements*, volume 1846 of *Lecture Notes in Mathematics*. Springer-Verlag, Berlin, 2004.

[7] H. Ammari and A. Khelifi. Electromagnetic scattering by small dielectric inhomogeneities. *J. Math. Pures Appl. (9)*, 82(7):749–842, 2003.

[8] S. Amstutz. Sensitivity analysis with respect to a local perturbation of the material property. *Asymptot. Anal.*, 49(1-2):87–108, 2006.

[9] S. Amstutz. Topological sensitivity analysis for some nonlinear PDE systems. *J. Math. Pures Appl. (9)*, 85(4):540–557, 2006.

[10] S. Amstutz and H. Andrä. A new algorithm for topology optimization using a level-set method. *J. Comput. Phys.*, 216(2):573–588, 2006.

[11] S. Amstutz and M. Ciligot-Travain. Optimality conditions for topology optimization subject to a cone constraint. *Preprint 78, Université d'Avignon*, 2008.

[12] I. I. Argatov. Asymptotic models for the topological sensitivity of the energy functional. *Appl. Math. Lett.*, 22(1):19–23, 2009.

[13] M. P. Bendsøe and N. Kikuchi. Generating optimal topologies in structural design using a homogenization method. *Comput. Methods Appl. Mech. Engrg.*, 71(2):197–224, 1988.

[14] M. P. Bendsøe and O. Sigmund. *Topology optimization*. Springer-Verlag, Berlin, 2003. Theory, methods and applications.

[15] F. Bonnans. *Optimisation continue*. Dunod, Paris, 2006.

[16] M. Burger, B. Hackl, and W. Ring. Incorporating topological derivatives into level set methods. *J. Comput. Phys.*, 194(1):344–362, 2004.

[17] P. G. Ciarlet. *Introduction à l'analyse numérique matricielle et à l'optimisation*. Collection Mathématiques Appliquées pour la Maîtrise. [Collection of Applied Mathematics for the Master's Degree]. Masson, Paris, 1982.

[18] G. Cohen. *Convexité et optimisation*. Lecture notes, Ecole Nationale des Ponts et Chaussées.

[19] M. C. Delfour and J.-P. Zolésio. *Shapes and geometries*, volume 4 of *Advances in Design and Control*. Society for Industrial and Applied Mathematics (SIAM), Philadelphia, PA, 2001. Analysis, differential calculus, and optimization.

[20] K. Eppler, H. Harbrecht, and M. S. Mommer. A new fictitious domain method in shape optimization. *Comput. Optim. Appl.*, 40(2):281–298, 2008.

[21] H. Eschenauer, V. V. Kobolev, and A. Schumacher. Bubble method for topology and shape optimization of structures. *Structural optimization*, 8:42–51, 1994.
[22] R. A. Feijóo, A. A. Novotny, E. Taroco, and C. Padra. The topological derivative for the Poisson's problem. *Math. Models Methods Appl. Sci.*, 13(12):1825–1844, 2003.
[23] S. Garreau, P. Guillaume, and M. Masmoudi. The topological asymptotic for PDE systems: the elasticity case. *SIAM J. Control Optim.*, 39(6):1756–1778 (electronic), 2001.
[24] J. M. Martínez. A note on the theoretical convergence properties of the SIMP method. *Struct. Multidiscip. Optim.*, 29(4):319–323, 2005.
[25] F. Murat and J. Simon. Quelques résultats sur le contrôle par un domaine géométrique. *Publ. Laboratoire d'Analyse Numérique, Université Paris 6*, pages 1–46, 1974.
[26] S. A. Nazarov and J. Sokołowski. Asymptotic analysis of shape functionals. *J. Math. Pures Appl. (9)*, 82(2):125–196, 2003.
[27] S. A. Nazarov and J. Sokolowski. Shape sensitivity of eigenvalues revisited. *Control and Cybernetics*, 37(4):999–1012, 2008.
[28] S. A. Nazarov and J. Sokolowski. Spectral problems in the shape optimisation. Singular boundary perturbations. *Asymptot. Anal.*, 56(3-4):159–204, 2008.
[29] J. Sokołowski and A. Żochowski. On the topological derivative in shape optimization. *SIAM J. Control Optim.*, 37(4):1251–1272 (electronic), 1999.
[30] J. Sokołowski and A. Żochowski. Optimality conditions for simultaneous topology and shape optimization. *SIAM J. Control Optim.*, 42(4):1198–1221 (electronic), 2003.
[31] J. Sokołowski and J.-P. Zolésio. *Introduction to shape optimization*, volume 16 of *Springer Series in Computational Mathematics*. Springer-Verlag, Berlin, 1992. Shape sensitivity analysis.
[32] M. Y. Wang, X. Wang, and D. Guo. A level set method for structural topology optimization. *Comput. Methods Appl. Mech. Engrg.*, 192(1-2):227–246, 2003.

Laboratoire d'analyse non linéaire et géométrie, Faculté des Sciences, 33 rue Louis Pasteur, 84000 Avignon, France.

E-mail address: samuel.amstutz@univ-avignon.fr